

Support Information

π -d conjugation regulates the cathode/electrolyte interface in all-solid-state lithium-ion batteries

Surong Zheng^{a,b,‡}, Shiwei Yu^{a,b,‡}, Zaka Ullah^c, Lei Liu^a, Ledi Chen^a, Houliang Sun^a,
Mingliang Chen^a, Liwei Liu^{a,*}, Qi Li^{a,*}

^a Key Laboratory of Nanodevices and Applications & Collaborative Innovation Center of Suzhou Nano Science and Technology, Suzhou Institute of Nano-Tech and Nano-Bionics, Chinese Academy of Sciences, Suzhou, Jiangsu 215123, China

^b Nano Science and Technology Institute, University of Science and Technology of China, Suzhou, Jiangsu 215123, China

^c Department of Physics, Division of Science and Technology, University of Education, Lahore 54770, Pakistan

* Corresponding authors: (Q. Li) qli2013@sinano.ac.cn; (L. Liu)

lwliu2007@sinano.ac.cn;

‡ These authors contributed equally to this work.

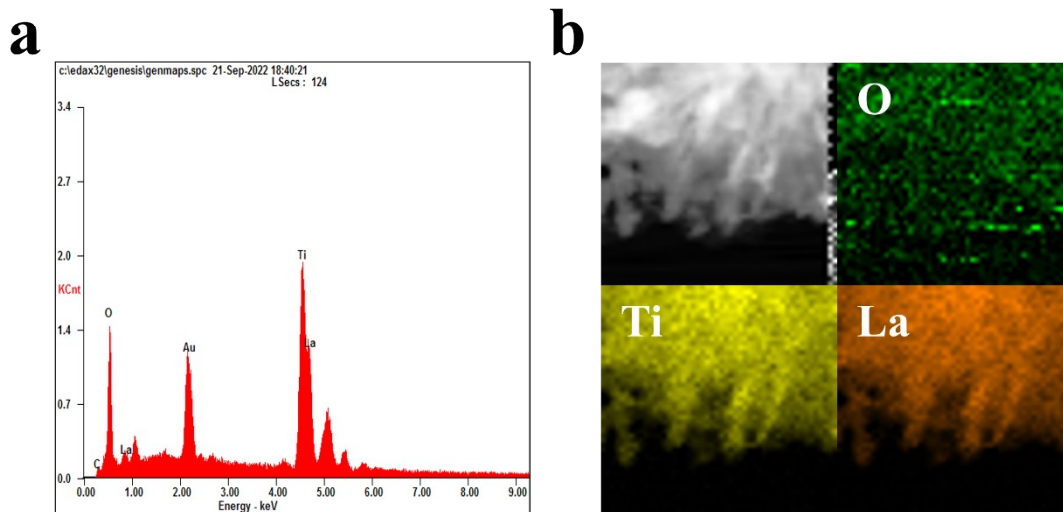


Figure S1. The spectrum of energy dispersive spectroscopy (a) and elemental map (b) of LLTO.

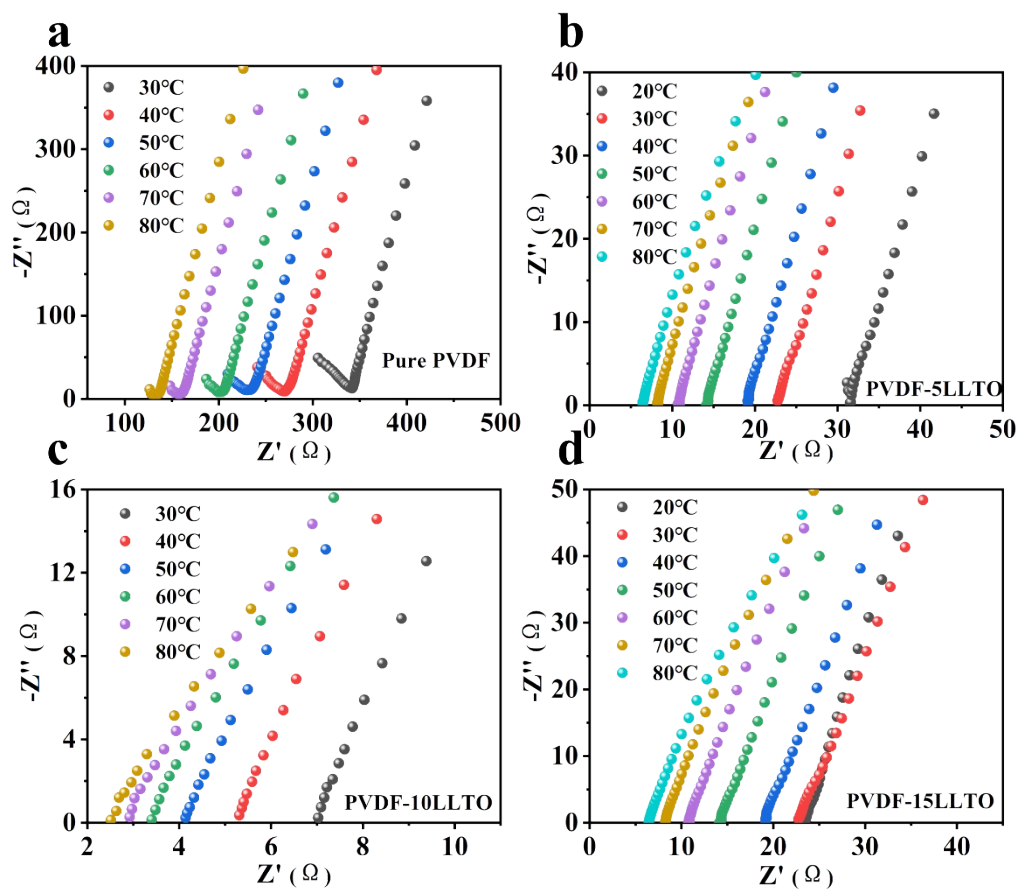


Figure S2. EIS curves of (a) Pure PVDF, (b) PVDF-5LLTO, (c) PVDF-10LLTO and (d) PVDF-15LLTO at different temperatures.

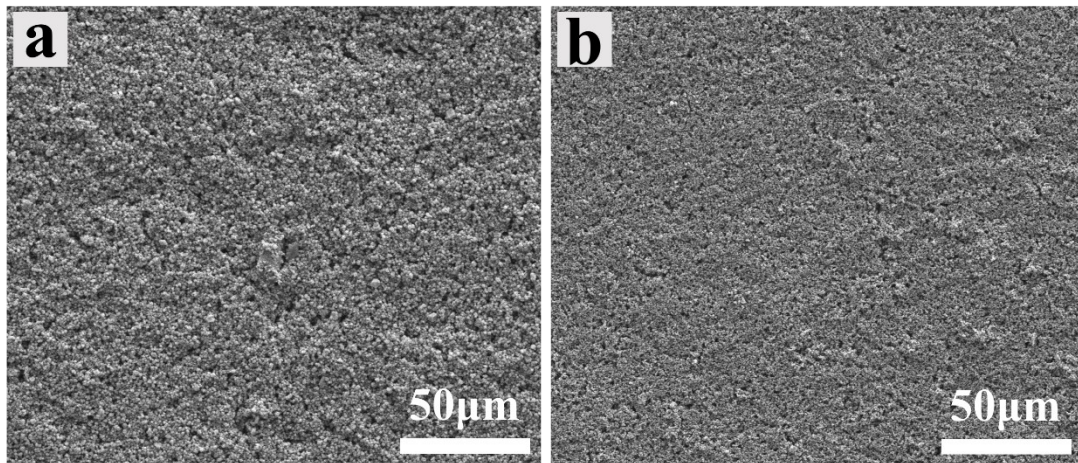


Figure S3. SEM micrographs of (a) PVDF-5LLTO and (b) PVDF-15LLTO electrolytes.

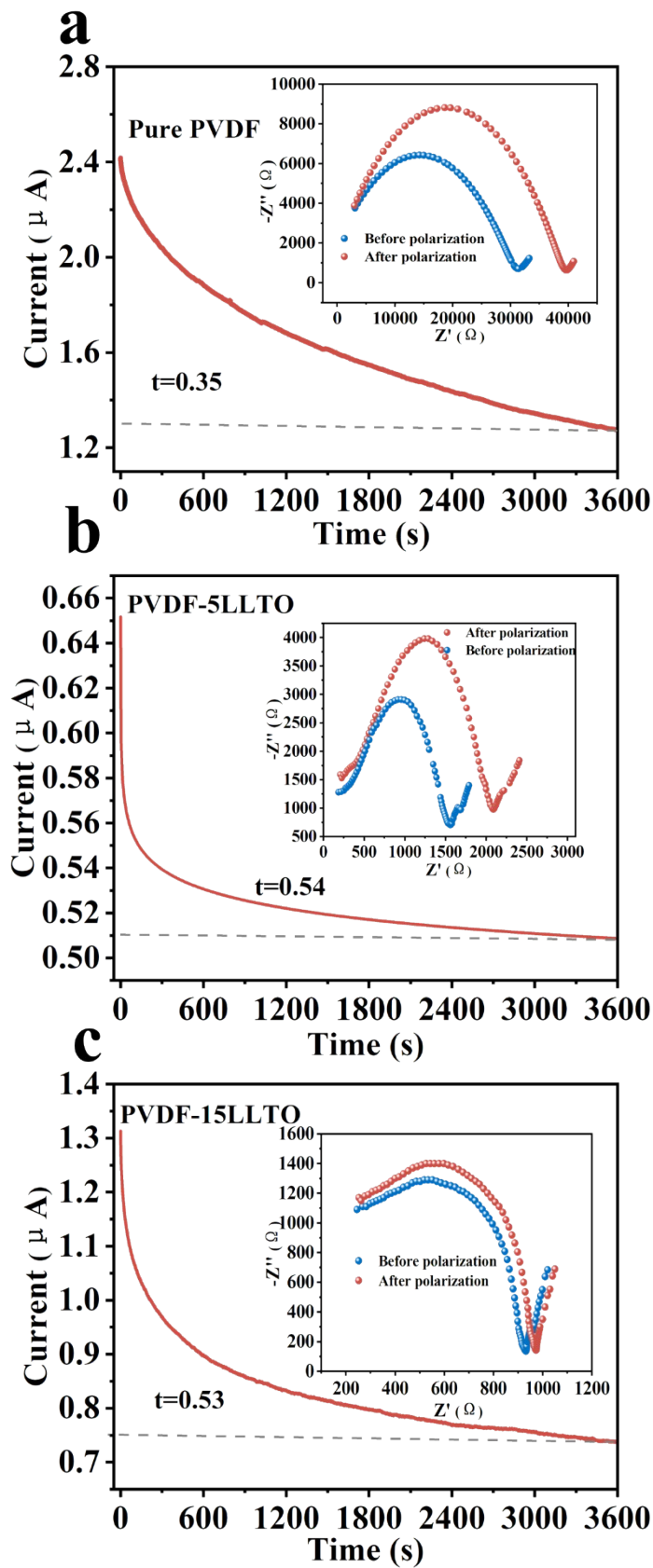


Figure S4. Polarization curves, and initial and steady-state impedance diagrams of (a) Pure PVDF, (b) PVDF-5LLTO and (c) PVDF-15LLTO CPEs.

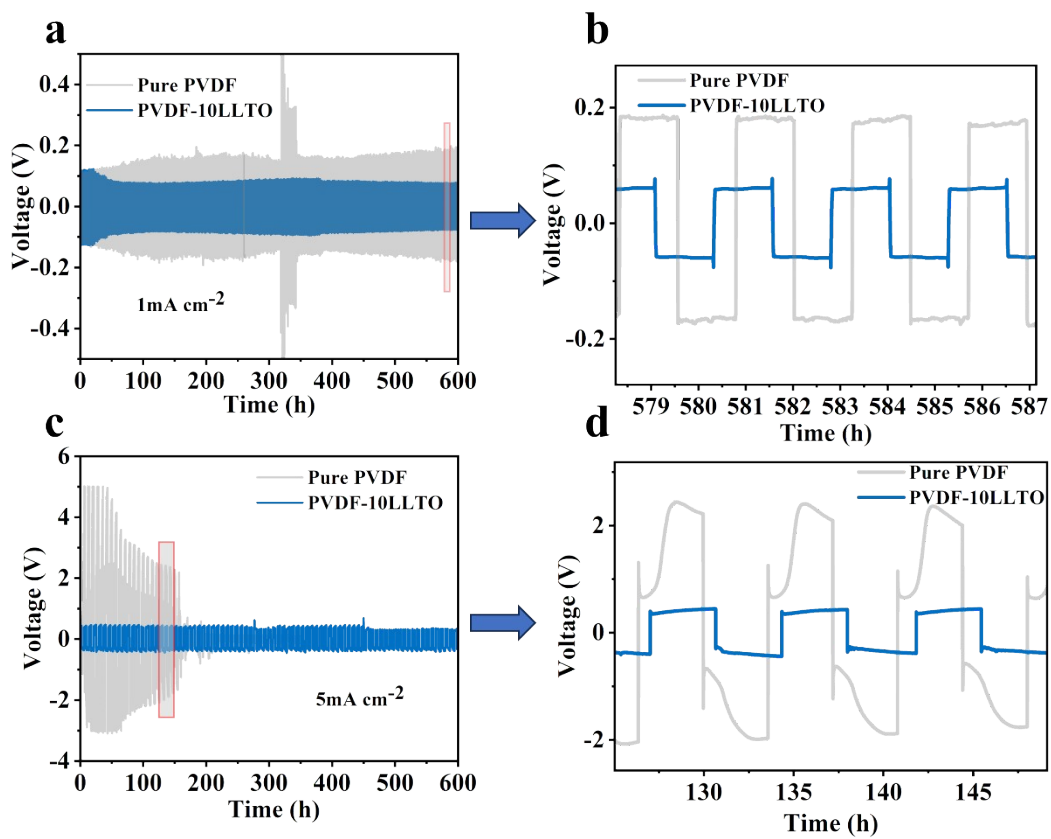


Figure S5. The charge-discharge performance diagram and its partial enlarged view with Pure PVDF and PVDF-10LLTO electrolytes at stripping/plating capacity of 1 mAh cm^{-2} and current density as (a, b) 1 mA cm^{-2} and (c, d) 5 mA cm^{-2} .

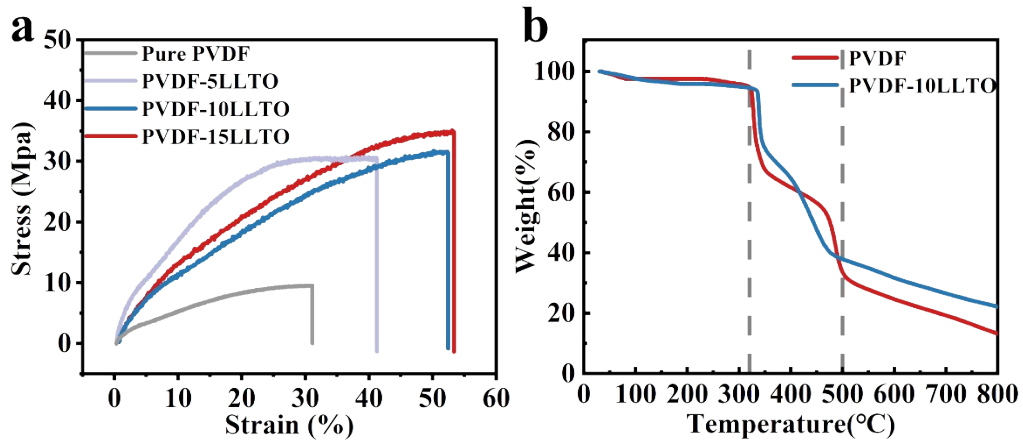


Figure S6. (a) Stress-Strain curve of PVDF-LLTO solid state electrolyte; (b) TG curve of Pure PVDF and PVDF-10LLTO.

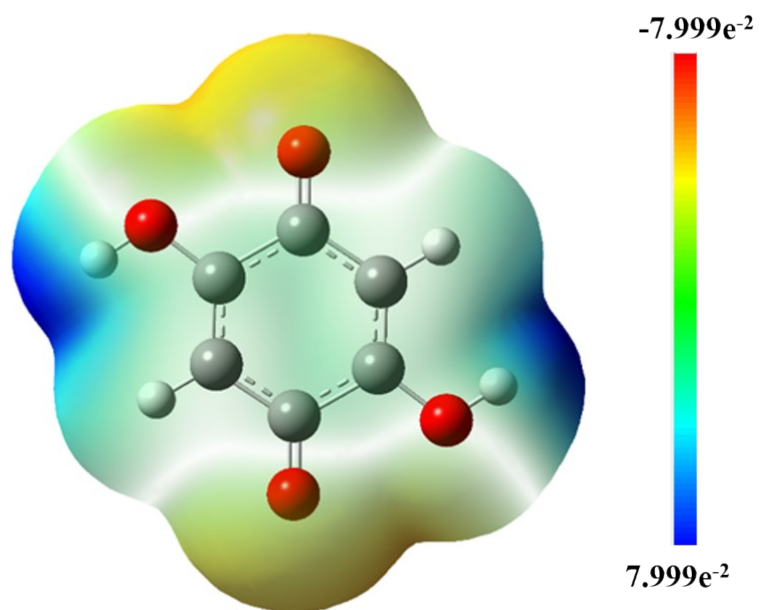


Figure S7. Static potential diagram of DHBQ; The calculations were carried out using Gaussian 09 program package. In order to better describe the bond structure, b3lyp functional combined with 6-31g(d) basis set was selected for geometry optimizations.¹

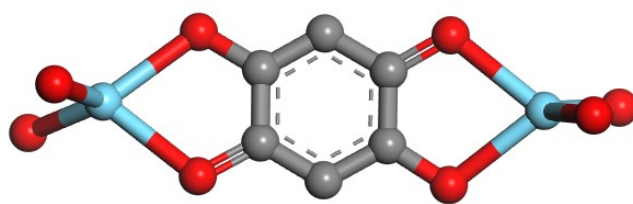


Figure S8. The π -d coordination structure.

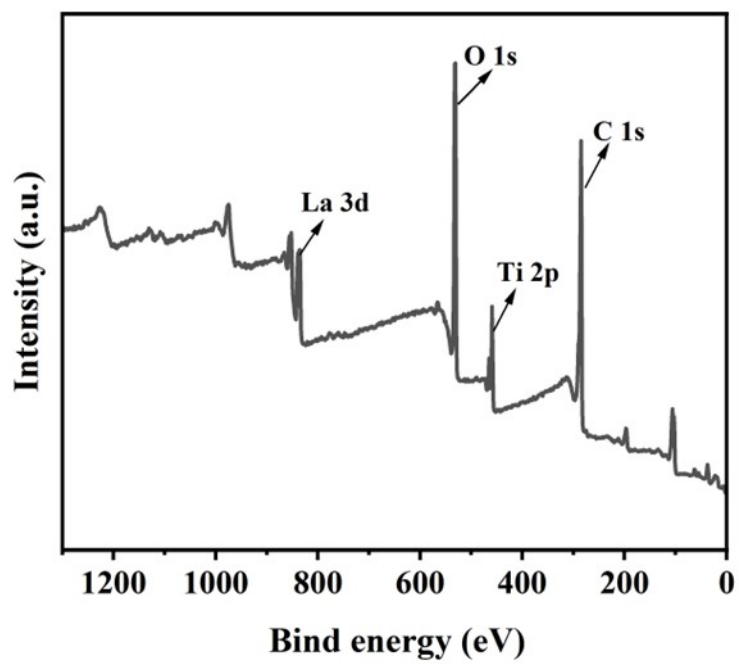


Figure S9. Full XPS spectra of DHBQ-LLTO.

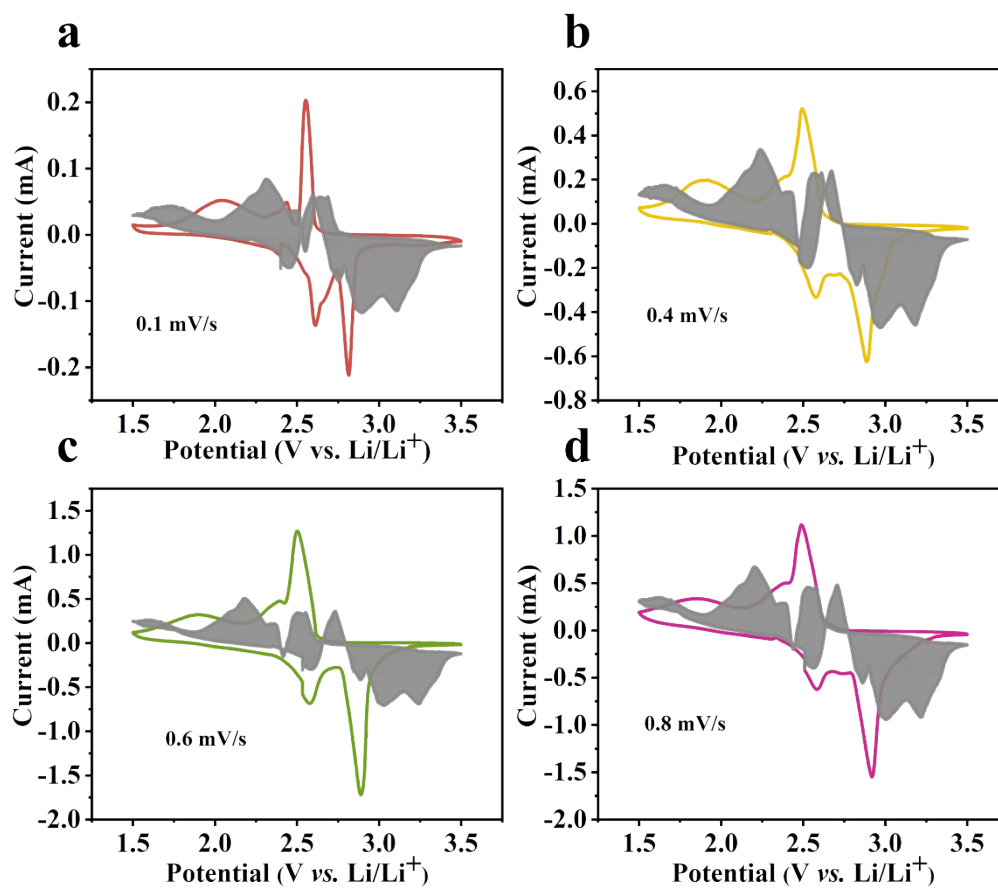


Figure S10. Capacitive contribution at (a) 0.1, (b) 0.4, (c) 0.6 and (d) 0.8 mV s⁻¹.

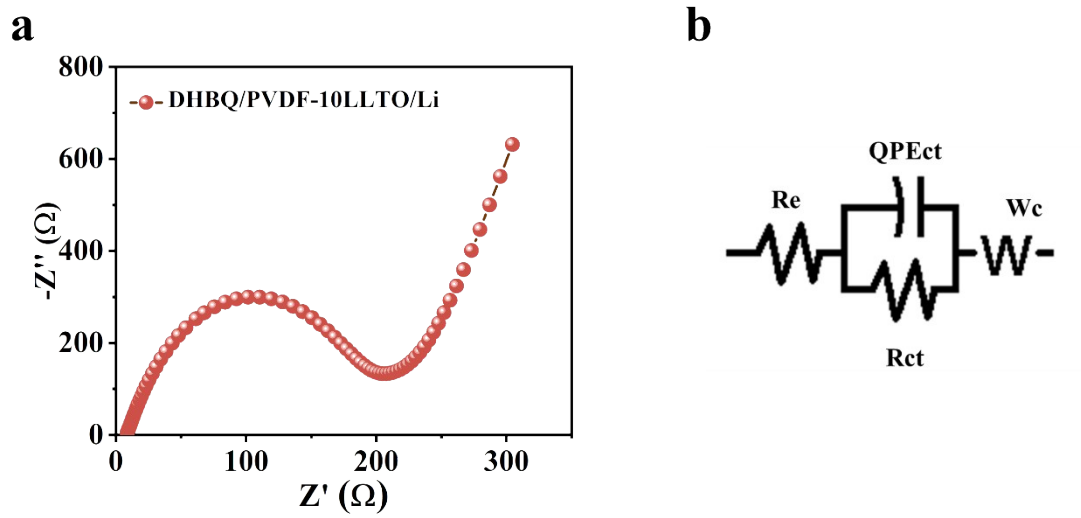


Figure S11. (a) AC impedance spectrum of DHBQ/PVDF-LLTO/Li ASSLB and (b) equivalent circuit diagram corresponding to AC impedance spectra.

Table S1. The element content of LLTO

Element	Wt%	At%
OK	24.66	65.69
AuM	15.32	03.32
TiK	21.58	19.20
LaL	38.44	11.79
Matrix	Correction	ZAF

Table S2. Ionic conductivity of Pure PVDF, PVDF-5LLTO, PVDF-10LLTO, PVDF-15LLTO CPEs at different temperatures.

Temperature	Pure PVDF	PVDF-5LLTO	PVDF-10LLTO	PVDF-15LLTO
30°C (S cm ⁻¹)	3.17×10 ⁻⁵	2.57×10 ⁻⁴	1.69×10 ⁻³	4.03×10 ⁻⁴
40°C (S cm ⁻¹)	9.12×10 ⁻⁵	3.24×10 ⁻⁴	2.24×10 ⁻³	4.67×10 ⁻⁴
50°C (S cm ⁻¹)	1.07×10 ⁻⁴	4.30×10 ⁻⁴	2.88×10 ⁻³	6.34×10 ⁻⁴
60°C (S cm ⁻¹)	1.23×10 ⁻⁴	5.12×10 ⁻⁴	3.50×10 ⁻³	8.45×10 ⁻⁴
70°C (S cm ⁻¹)	1.56×10 ⁻⁴	7.23×10 ⁻⁴	4.06×10 ⁻³	1.10×10 ⁻³
80°C (S cm ⁻¹)	1.86×10 ⁻⁴	9.38×10 ⁻⁴	4.74×10 ⁻³	1.41×10 ⁻³

Table S3. Activation energy of Pure PVDF, PVDF-5LLTO, PVDF-10LLTO, PVDF-15LLTO CPEs.

	Pure PVDF	PVDF-5LLTO	PVDF-10LLTO	PVDF-15LLTO
Ea (eV)	0.287	0.241	0.191	0.242

Reference:

[1] M. J. Frisch, G. W. Trucks, H. B. Schlegel, G. E. Scuseria, M. A. Robb J. R. Cheeseman, G. Scalmani, V. Barone, B. Mennucci, G. A. Petersson, et al, Gaussian 09, Revision D.01, Gaussian, Inc., Wallingford CT, 2013.